

Recovery of value-added compounds through fast pyrolysis of apple pomace hydrochar

Madeline Karod ^a, Kellene A. Orton ^b, Yaseen Elkasabi ^c, Charles A. Mullen ^c, Anne E. Harman-Ware ^b, Kristiina Iisa ^b, Jillian L. Goldfarb ^{a,d,*}

^a Department of Biological & Environmental Engineering, Cornell University, 111 Wing Drive, Ithaca, NY 14853, USA

^b National Renewable Energy Laboratory, 15013 Denver West Parkway, Golden, CO 80401, USA

^c USDA-Agricultural Research Service, Eastern Regional Research Center, 600 E. Mermaid Lane, Wyndmoor, PA 19038, USA

^d Smith School of Chemical & Biomolecular Engineering, Cornell University, 113 Ho Plaza, Ithaca, NY 14853, USA

ARTICLE INFO

Keywords:

Fast pyrolysis
Hydrothermal carbonization
Molecular beam mass spectrometry (MBMS)
Hydrochar
Secondary char
Primary char

ABSTRACT

The environmental challenges associated with food production can be addressed via the thermochemical upcycling of agro-industrial biomass. Two such methods, hydrothermal carbonization (HTC) and pyrolysis, can be coupled to first reduce the water content of wet biomass wastes by producing a hydrochar (HC) via HTC and then a bio-oil via pyrolysis of the HC. However, HTC of biomass results in the formation of secondary char (SC), an amorphous tar-like mixture resulting from organic compounds released into the aqueous phase that adsorb, recondense and polymerize on the parent biomass. This study investigated how HTC temperature impacts the formation of SC from apple pomace and the SC's subsequent impact on fast pyrolysis products. HCs were produced at temperatures of 175°C, 200°C, and 250°C. Lower HTC temperatures favor the formation of biorefinery platform chemicals such as 5-hydroxymethylfurfural and levulinic acid, while higher temperatures result in increased lignin degradation products (i.e., phenolics). HCs were subjected to fast pyrolysis before and after SC extraction in two analytical pyrolysis instruments. Fast pyrolysis of HC produced compounds similar to those found in SC, but with variations in CO and CO₂ emissions. The combination of SC extraction and fast pyrolysis demonstrates promise for recovering value-added compounds from agro-industrial waste biomass while retaining a solid char for fuel and carbon management.

1. Introduction

Upcycling agro-industrial waste is vital to mitigate the environmental impacts of modern agricultural and food production practices [1]. By recovering biomass destined for landfills, carbon can be reclaimed to produce value-added compounds [2]. Thermochemical conversion processes offer promising solutions to convert biomass carbon into sustainable fuels or valuable chemicals and occur orders of magnitude faster than anaerobic digestion that produces relatively low-value methane [3,4].

The choice of thermochemical treatment process depends on feedstock properties and treatment objectives. Hydrothermal carbonization (HTC) is often chosen to produce char from wet wastes. Because HTC occurs in an aqueous environment, a drying step is not required [5]. Pyrolysis is the more commonly chosen thermochemical conversion process but requires a step in which latent moisture content is removed

before pyrolysis [6]. During fast pyrolysis, heating rates range between 10 and 10,000 °C/min with a residence time of mere seconds [16]. The bio-oil yield is higher from fast pyrolysis than from slow pyrolysis (residence times range from minutes to hours), but a very dry biomass, (with a moisture content < 10 %) is ideal [17,18]. Pyrolysis, specifically fast pyrolysis, is more commonly elected to produce bio-oil, while HTC (temperature ranging from 175 to 250°C) is typically utilized to produce a solid hydrochar (HC). Both treatments concentrate fixed carbon into a solid char, but due to the closed-system reactor that is used in HTC, a portion of the compounds that are initially hydrolyzed from the biomass into the water phase undergo condensation and polymerization reactions to form a secondary layer of char (secondary char, SC) on the surface of the primary layer of char [7] (primary char, PC). We note that SC is a complex amorphous mixture that contains products of secondary polymerization reactions as well as hydrolyzed compounds adsorbed from the liquid phase. Preliminary studies show that HC poses a threat to

* Corresponding author at: Smith School of Chemical & Biomolecular Engineering, Cornell University, 113 Ho Plaza, Ithaca, NY 14853, USA.
E-mail address: goldfarb@cornell.edu (J.L. Goldfarb).

the environment when applied to land, as it is potentially phytotoxic (an effect ascribed to the SC [8]). However, several papers have acknowledged that by extracting SC from HC, PC can be isolated and is more inert, showing properties more akin to a biochar which is often used in environmental applications. Isolated SC contains compounds that may have value in other fields [7,9–11].

Hydrochar was previously explored as a feedstock for pyrolysis in a cascading thermochemical conversion pathway [12,13]. Pyrolyzing HCs causes devolatilization of both the carbonaceous matrix and the semi-volatile SC on the surface, all of which can be condensed into a bio-oil. Few studies have investigated fast pyrolysis of HC. One demonstrated that cellulosic HC can produce value-added compounds during fast pyrolysis, including furans, which can form polyfuranics via polycondensation and polymerization reactions [14]. Another study using almond shell hydrochar found that fast pyrolysis at 500°C for 15 s produced a valuable bio-oil consisting of phenolics and sugars, indicating that valuable compounds can be retrieved from this cascading thermochemical pathway [15].

However, no study to date has attempted to deconvolute the devolatilization of secondary char (SC) from other pyrolytic reactions that occur during pyrolysis of HC. We hypothesize that valuable compounds present in the SC can be concentrated by either solvent or pyrolytic extraction; as such, we set out to investigate the devolatilization of these compounds during fast pyrolysis in a quantitative manner. The motivation for SC extraction was two-fold: first, to determine the composition of SC and to understand the role SC devolatilization plays in HC pyrolysis, separate from that of PC pyrolysis. Second, to determine if extracting the SC before pyrolysis yields value-added compounds (in the SC extract) and impacts the pyrolysis bio-oil. In this study, SC was extracted from HC before analytical fast pyrolysis to investigate the composition of the pyrolysis products when PC is pyrolyzed, as compared to pyrolysis of HC. Using analytical fast pyrolysis, the formation of pyrolysis vapors was quantified to determine their composition as a function of HTC process conditions. Although chemical extraction informs us of the composition of SC, it cannot shed light on the compounds that are devolatilized when SC undergoes pyrolysis – a critical question to ask in the context of compound recovery. The composition of vapors released from hydrochar were examined, both before and after SC extraction, by pyrolyzing HC and post-extraction PC, to determine the degree to which SC influences the compounds within the vapors.

2. Methods and materials

Apple pomace (AP) was produced using Ruby Frost apples (*Malus domestica*) grown in New York State, which were cored, pulverized, and pressed to make AP. AP was stored at -4°C and thawed prior to experimentation. AP was hydrothermally carbonized at three temperatures (and one residence time). The HCs were characterized and a portion of each subjected to solvent extraction and analysis. The HCs were subjected to three different analytical pyrolysis techniques. An

experimental flowchart is shown in Fig. 1; method details are provided below.

2.1. Hydrothermal carbonization of AP

AP was carbonized in a 1-L Parr Series 4525 Bench Reactor equipped with a 4848 Parr Controller at Cornell University in Ithaca, NY. Experiments were performed at either 175°C, 200°C, or 250°C, with a residence time at final temperature of 2 hours. The AP was loaded into the reactor with deionized water at a ratio of 15 % dry biomass to 85 % water. The reactor was flushed three times with high purity nitrogen and then pressurized with nitrogen to 0.55–0.57 MPa to eliminate oxygen from the system. The reactor was heated to temperature at an average heating rate of 2.6 °C/min. These temperatures were chosen to test within the bounds of hydrothermal carbonization (175–250°C). Upon reaching 60°C, the reactor was set to stir at 400 RPM. After a hold of 2 hours at the reaction temperature, the reactor was rapidly cooled using an ice bath and then depressurized. The hydrochar and process water were separated using vacuum filtration on a cellulose filter paper (Whatman, 45 µm). The mass of HC was recorded to determine the yield and the gas yield was calculated by applying the ideal gas law, using the difference in pressure before HTC and after quenching. Liquid yield was calculated by difference.

2.2. Secondary char extraction and analysis

Secondary char extraction was performed using dichloromethane (DCM) in a Dionex 350 Accelerated Solvent Extractor (ASE, Thermo-Fisher). For mass balance purposes, 10 mL extraction cells and a cellulose filter were pre-weighed, after which 0.50 g of AP HC were added. The cell was sealed and placed in the autosampler. The programmed method for extraction was as follows: the cell was heated to 100 °C during two 5-minute extraction cycles with a static time of 4 minutes in between. During each cycle, 10 mL of DCM was pumped through the cell at 10.34 MPa (1500 PSI). Over two cycles, the total DCM use was 20 mL. After the cell cooled, it was placed in an oven overnight at 80 °C and the final mass of primary char, cell and filter paper was recorded. The mass of the SC was determined by difference. The extracted SC was stored in glass vials in the refrigerator (at 4°C) prior to analysis.

1 mL of the extracted secondary char in DCM was added to a vial for compositional analysis via Gas Chromatography-Mass Spectroscopy (GC-MS). A Shimadzu GC 2010 Plus GC-MS with a Restek Rtx-5sil MS 30 m fused silica column was used for compound detection and quantification of the SC. Samples were run on a split ratio of 10:1, and the GC-MS was programmed with a column oven temperature of 40 °C, injection temperature of 280 °C, ion source temperature of 230 °C, and interface temperature of 320 °C. The oven temperature started at 40 °C, was held for 6 minutes, ramped to 300 °C at 5 °C/min where it was held for 5 minutes, and then cooled at a rate of 20 °C/min to 250 °C before cooling to ambient conditions. The compounds detected by the MS were identified using a NIST library with at least 70 % match and quantified by area counts using a calibration of 89 compounds often seen in treated lignocellulosic biomass. An open-source Python code was used for data analysis published by Pecchi and Goldfarb [19].

2.3. Solids characterization

Proximate analysis was performed using approximately 6 mg of sample added to 70 µL ceramic crucibles in a TA Instruments Simultaneous Thermal Analyzer 650. Samples were heated at 50 °C/min under high purity nitrogen flowing at 100 mL/min to 110 °C and held for 30 minutes to remove moisture. The temperature was then increased at a rate of 10 °C/min to 900 °C and held for 30 minutes to determine volatile matter (VM) content. The gas was then switched to dry air flowing at 100 mL/min and the temperature ramped to 950 °C at 10 mL/min to determine fixed carbon (FC) content. Analyses were run

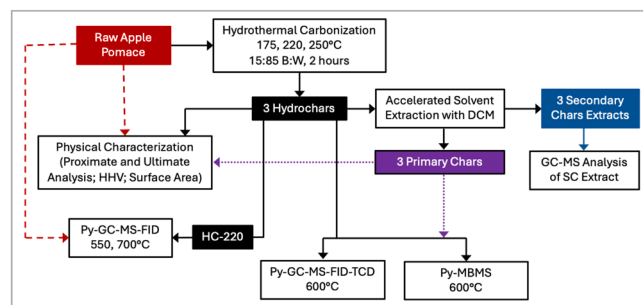


Fig. 1. Experimental flowchart to explore the impact of secondary char on fast pyrolysis of apple pomace hydrochars.

in triplicate.

Higher heating values (HHV) were determined according to CEN/TS 14918 standards using a Parr 6200 Calorimeter calibrated with benzoic acid. HC and PC samples were measured in triplicate. Raw-AP was excluded due to the slurry nature of the sample, with a moisture content of ~80 %. Energy yield (reported on dry basis) was determined from HHV values as follows [20]:

$$\text{Energy yield (\%)} = \text{HHV}_{\text{HC}} / \text{HHV}_{\text{Raw-AP}} * (\text{Solid yield \%}) \quad (1)$$

Ultimate analysis was performed on Raw-AP, HCs and PCs using a CE-440 Elemental Analyzer (Exeter Analytical Inc.) to determine the elemental composition (C, H, N, and O by difference; available in [Supplemental Information, SI](#)). The higher heating value (HHV) of the Raw-AP was calculated based on the elemental analysis (available in SI) according to the modified Dulong's Equation [21].

Surface areas of the char samples were analyzed on a Micromeritics 3Flex. Samples were degassed at 180 °C for 48 hours under vacuum prior to analysis. BET surface area was measured using five isotherm points between 0.05 and 0.30 relative pressure with confidence intervals reported based on the linear regression of BET curve fitting [22].

2.4. Analytical pyrolysis

Three unique analytical pyrolysis systems were used at two separate locations. At the National Renewable Energy Laboratory (NREL) in Golden, CO a tandem micro-furnace pyrolyzer (PY-2020iS, Frontier Laboratories, Japan) was coupled to an Agilent 7890/5974 GC-MS-FID-TCD. Approximately 500 µg of HC and PC samples were loaded into 80 µL stainless steel cups, which were placed into the autosampler which dispensed samples into the pyrolysis zone at 600 °C (with interface at 350 °C). Pyrolytic vapors were carried in He flowing at 54 mL/min over a liquid nitrogen trap to collect the condensable vapors. Non-condensable vapors were carried into a GS-GasPro column and were measured by a thermal conductive detector (TCD). The condensed vapors were separated in an Ultra-Alloy-5 capillary column that utilized a stationary phase of 5 % phenyl and 95 % dimethyl polysiloxane. The GC oven was programmed to hold at 40 °C for 3 minutes and then ramped to 240 °C at a rate of 6 °C/min. A NIST library was used to identify the compounds and quantification was performed using FID, which was calibrated with nonane and checked against several other short-chain alkanes. A response factor was calculated for 42 compounds based on the effective carbon number, as described in Scanlon and Willis (1985) [23]. The TCD and MS were calibrated by area to quantify CO and CO₂, respectively.

Pyrolysis-molecular beam mass spectrometry (Py-MBMS) was also used at NREL to analyze pyrolysis vapors from HCs and PCs [24–26]. Approximately 5 mg of sample was added to an 80 µL stainless steel crucible and loaded onto an autosampler. The sample was then introduced to a quartz pyrolysis reactor at 600°C with a 0.9 L/min helium carrier gas flow. MS data was recorded at *m/z* 30–450 over 60 s using 17 eV electron impact ionization. Data was taken in triplicate. MS data was acquired using an Extrel Super-Sonic MBMS Model Max 1000 and then processed using Merlin Automation Software (V3).

At USDA-ARS Eastern Regional Research Center in Wyndmoor, PA, micropyrolysis experiments were conducted on hydrochar produced at 200°C (AP-HC-200) and raw apple pomace (AP-Raw). A Frontier Lab Double-Shot micro pyrolyzer PY-3030iD with a Frontier Lab Auto-Shot Sampler AS-1020E, with a Shimadzu GC-2020 GC-MS-FID attached was coupled with a catalytic microreactor (Polyarc, Activated Research Company), which converted all organic compounds to methane for universal response detection by a flame ionization detected (FID), and used to quantify volatiles from pyrolysis. Separately, a Py-GC-MS was used to identify the compounds in the pyrolysis vapors. For this analysis, 500 µg of sample was added to a steel cup that was loaded into the autosampler, which dropped the sample into a micropyrolyzer (Multi-

Shot Pyrolyzer EGA/PY 3030D, Frontier Laboratories Ltd), which was connected inline to a GC. A 2.5 mL/min flow of He was used as a carrier gas and the volatiles were sent through a Restek RTX-1701 GC column with 0.25 mm ID x 60 m length and a 0.25 µm film thickness. The inlet temperature was held at 280 °C and a split ratio of 30:1 was used. The column oven was initially held at 45 °C for 4 minutes and then heated at 3 °C/min to 280 °C, where it was held for 20 minutes. The Polyarc reactor was heated to 300 °C. Compounds were detected by the FID at 300 °C with a hydrogen flow rate of 1.5 mL/min and an air flow rate of 350 mL/min. AP-Raw was pyrolyzed at 550 °C and HC-200 was pyrolyzed at 550°C and 700 °C, all in triplicate. A NIST library was used to identify compounds. Quantification was done using integrated peak areas which was quantified relative to the integrated peak area of o-cresol, an external standard.

3. Results and discussion

Apple pomace (AP) underwent HTC at three temperatures: 175, 200, and 250°C, and the resulting HCs underwent SC extraction to isolate PC as a solid and SC in a DCM liquid phase. The HCs and PCs underwent fast pyrolysis at 600°C to quantitatively determine the composition of volatile and semivolatile compounds produced. AP Samples were named using their status as HC, PC, or SC and the carbonization temperature; i.e., HC-175 or PC-175, etc.

3.1. Hydrochar and primary char yields and properties

The yields of HC ([Table 1](#)) show that as temperature increased, solid (HC) yield decreased, and gas and liquid yields increased. The gas is expected to be a mixture of predominantly CO₂ and some CO as decarbonylation, decarboxylation, and deoxygenation reactions proceed during HTC [27,28]. The liquid phase was not a focus of this study, but as an aqueous solution enriched with carbon, it may have applications in chemical and nutrient recovery or recirculated in further HTC experiments [29], and will be more thoroughly discussed in future work.

Higher heating value (HHV) quantifies the energy density of the samples in MJ/kg hydrochar while the energy yield shows the amount of energy in the feedstock that was recovered post-HTC and SC extraction. Shown in [Table 1](#), the HHVs and the energy yields increase with HTC temperature and decrease post-SC extraction compared to HC equivalents. The HHV of HC-250 is notable at 35.55 MJ/kg, as it is very near to the energy density of bituminous coals, which can range from 35 to 45 MJ/kg [30]. The HHV values are all statistically significantly different from the Raw-AP (p-value <.01, two-tailed t-test of pairwise data), and the HCs all show significant differences from one another. The HHV of HC and PC produced at 200°C are not statistically significantly different, which may indicate that SC extraction both isolates valuable compounds from the HC and retains the energy density in the PC. PC-200 also has the lowest yield (12.90 ± 0.98 wt%) which may be a factor in the high retained energy density. The energy densities of HC- and PC-175 as well as HC- and PC-250 are both significantly different from each other, which indicates that removing SC from the HC (with the exception of 200°C) removes valuable materials from an energy perspective, but it may also indicate that the compounds in SC have value as isolated compounds in other applications.

Raw AP, HCs and PCs were characterized via thermogravimetric analysis to determine volatile matter (VM) and fixed carbon (FC) content, as shown in [Fig. 2](#). The proximate analysis results show Raw AP to have the lowest FC content, and both high VM and ash content (provided in SI). As HTC temperature increases, FC increases. Additionally, FC content increases and VM decreases post-SC extraction; however, only HC-175 and PC-175 show statistically significant differences (p-value < 0.05) among these data.

Values are shown as an average of three replicates ± one standard deviation.

Table 1

HTC and secondary char extraction yields reported on a dry AP basis and HC basis, respectively. Liquid yields calculated by difference for both HC and PC. Heating values of raw AP and HC, PCs. Values are reported as an average of three samples \pm one standard deviation.

	HTC and Extraction Yields (wt%)						HHV (MJ/kg) of Solid	Energy Yield (% feedstock basis)	
	Solid		Liquid		Gas				
<i>As-Carbonized Hydrochar Yields</i>									
Raw	-	-	-	-	-	-	-	-	
HC-175	49.3	\pm	1.7	49.5	\pm	1.4	1.3	\pm 18.14	
HC-200	48.6	\pm	7.0	47.2	\pm	7.1	4.2	\pm 22.92	
HC-250	43.1	\pm	2.1	50.4	\pm	2.4	6.5	\pm 0.2 25.79	
PC-175	76.64	\pm	3.12	23.36	\pm	3.12	-	\pm 0.4 35.55	
PC-200	87.10	\pm	0.98	12.90	\pm	0.98	-	\pm 0.85 0.43	
PC-250	85.46	\pm	2.01	14.54	\pm	2.01	-	\pm 0.87 0.42	
								85 % 69 %	
<i>Secondary Char Extraction Yields</i>									
PC-175	76.64	\pm	3.12	23.36	\pm	3.12	-	\pm 0.31 45 %	
PC-200	87.10	\pm	0.98	12.90	\pm	0.98	-	\pm 0.87 59 %	
PC-250	85.46	\pm	2.01	14.54	\pm	2.01	-	\pm 1.14 64 %	

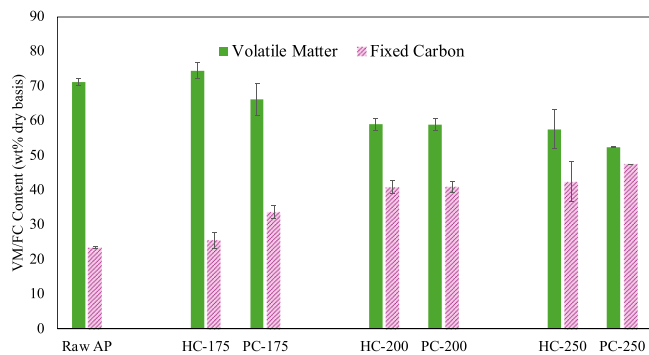


Fig. 2. Volatile matter and fixed carbon content on a dry basis of the AP-Raw, HC, and PCs.

3.2. Secondary char composition

The secondary char composition as analyzed by GC-MS (Fig. 3) highlights the impact of HTC temperature on SC formation and condensation of organics on the surface of primary char. At low carbonization temperatures, 5-hydroxymethylfurfural (5-HMF) is dominant as it is the main dehydration product of glucose [31]. As the 5-HMF further degrades it decomposes into a mixture of carbonyls (aldehydes and ketones) and levulinic acid, a C5 short-chain acid resulting from the furan ring opening. At higher temperatures, 5-HMF compounds merge together via alpha-carbons to form the carbonaceous scaffold of hydrochar in the form of a polyfuran [32]. The concentration of 5-HMF

decreases as the temperature increases, with AP-175 having 17 wt% 5-HMF, AP-200 having 11 w%, and AP-250 having 0.43 wt%, while levulinic acid concentration increases from 0.19 wt% to 0.52 wt% to 1.68 wt% as the carbonization temperature increases. Fatty acids are present in apple skin [33] and are present in concentrations of 2 %, 4 %, and 3 %, for AP-175, 200, 250, respectively. Pecchi et al. [34] found the hydrolysis of triglycerides to be correlated with carbonization temperature up until 250°C, at which point reactions proceed without kinetic limitations. Here, the fatty acid content in AP-200 and AP-250 is not significantly different ($p>0.05$), nor is the fatty acid content in AP-175 and AP-250, so no conclusions can be drawn with regards to any difference in fatty acid concentration with increased carbonization temperatures. Phenols and other aromatics present in AP-SC-250 are likely due to a breakdown of the lignin content of the AP [35], which can be found in the range of 15–23 % [36]. The total yield displayed in Fig. 3 represents the percent of the SC that was detected via GC-MS.

SC recovery appears to decrease with carbonization temperature (statistically significantly different between SC-175, SC-200 and SC-250). As the extraction was performed with DCM, it is possible that the compounds present in the SC from higher temperatures were insoluble due to increased polarity or they consisted of molecules that are not detectable via GC-MS due to boiling point.

3.3. Pyrolysis product composition as determined by Py-GC-MS

Analytical pyrolysis allows for pyrolysis vapor identification *in situ* and is useful for analysis of pyrolysis products. The compounds devolatilized during HC and PC pyrolysis were identified by a MS and then quantified using FID and a set of standards. Composition and total

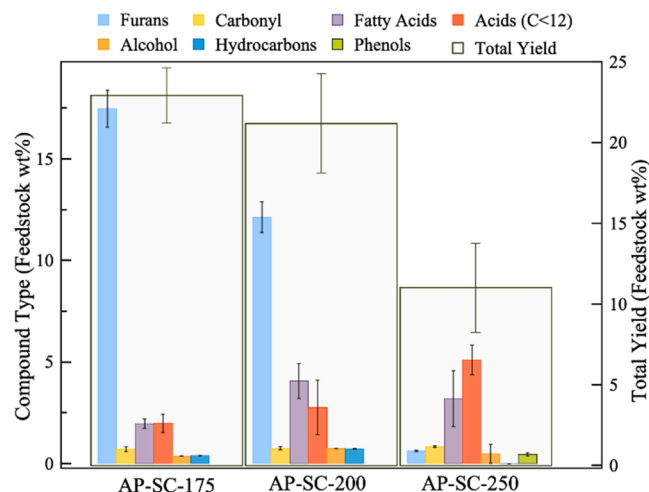


Fig. 3. GC-MS analysis of SC-175, 200, 250 extracted in DCM, shown as functional groups detected on the basis of wt% of SC. Reported as an average of three triplicates \pm one standard deviation.

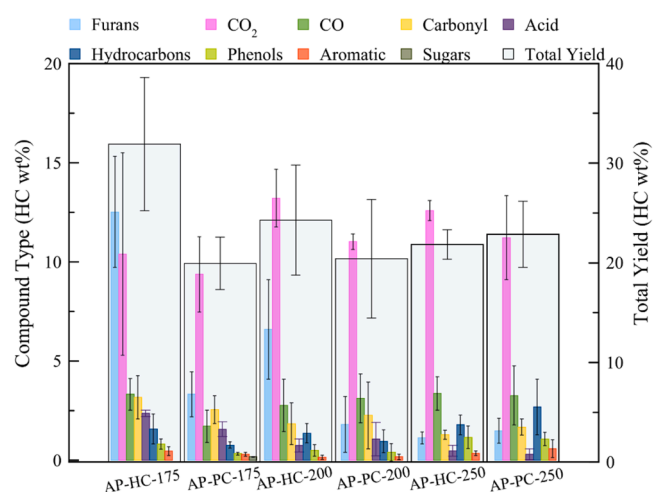


Fig. 4. Pyrolysis vapors as determined by Py-GC-MS-FID-TCD at 600°C. Reported on a HC-wt% basis. Values are reported as an average of three samples \pm one standard deviation.

detectable yield of pyrolysis vapors emitted from HC and PC are shown in Fig. 4. Values are provided on a basis of wt% hydrochar, to allow comparisons between the HC and PC that demonstrate the loss of compounds from the SC extraction. The use of TCD also allows for quantification of the CO that can be produced during pyrolytic cracking [37].

HC-175 and PC-175 show a total product identification of 30 % and 20 %, respectively. As PC makes up 75 % of HC, it appears that the change in detected compounds may be directly correlated to the compounds removed during SC extraction. Statistically, these two values show a significant difference in total product identification ($p < 0.05$). Yet, these samples show nearly identical CO and CO_2 emissions during fast pyrolysis, which indicates CO and CO_2 are formed from the pyrolysis of PC, whereas the SC devolatilization does not produce these gases. Instead, SC reactions may be dehydration or rehydration reactions or the formation of other small molecules that are not detected by the analytical equipment. Not surprisingly, the furans present in the low-temperature SC are devolatilized during this rapid pyrolysis; the furanic compound yield for PC-175 is almost 75 % lower than HC-175. Similarly, the relative amounts of phenols and acids decrease in bio-oil, and there's a slight increase in the relative abundance of carbonyls produced from PC-175 vs HC-175 due to extraction.

The HC-200 and PC-200 show a total product identification of 25 % and 20 %, respectively, though these values do not show a statistically significant difference ($p > 0.05$). The smaller difference in detected compounds from that of HC-175 and PC-175 may be due to the smaller amount of SC on the surface of HC-200 (12.9 %). For both 175 and 200 °C, there is a lower concentration of furans in the PC as they are extracted as SC. There is a significant difference between the CO_2

produced during HC and PC pyrolysis, which may be due to the increased acid concentration in the SC undergoing cracking reactions, producing CO_2 .

The HC-250 and PC-250 show a total product identification of 21 % and 23 %, respectively, though these values are not statistically significantly different from one another ($p > 0.05$). It is possible that there were few detectable compounds released from SC-250.

The data in Fig. 4 shows that AP carbonized at 175 °C has the most volatiles, likely due to the high 5-HMF content on surface of HC-175 as well as the relatively lower carbonization that occurs at 175 °C, versus 200 °C and 250 °C. As the carbonization temperature increases, furans are likely to either degrade into smaller compounds, including CO and CO_2 , or become part of the carbonaceous matrix as a polyfuran, which would point towards the decreased volatiles released during pyrolysis.

The MBMS data in Fig. 5a shows the mass normalized total ion count TIC (in TIC/g char) binned in groups of 30 m/z ratios from 30 to 450 m/z (Full spectra available in SI). The figure shows 175 °C HTC temperature to have increased volatilization compared to the other HTC temperatures, with the sum of mass-normalized intensities peaking at approximately 4×10^7 TIC/g char, while 200 °C and 250 °C show maximum TIC sums around 10×10^7 TIC/g char. The increased vapors detected from HC- and PC-175 are likely due to the increased volatile matter present in these samples. Spectra at 175 °C and 200 °C show the majority of pyrolysis vapors to have smaller m/z ratios, below 150 m/z , while HC and PC-250 had pyrolysis vapors that ranged from 30 to 250 m/z . This is likely due to the degradation of lignin that occurs at 250 °C, which ultimately allows for a higher aromatic content in the pyrolysis vapors. For instance, 2-methoxyphenol (m/z 124), eugenol (m/z 55, 91, 131), and coniferyl alcohol (m/z 179, 225) and aldehyde (m/z 147, 178) are

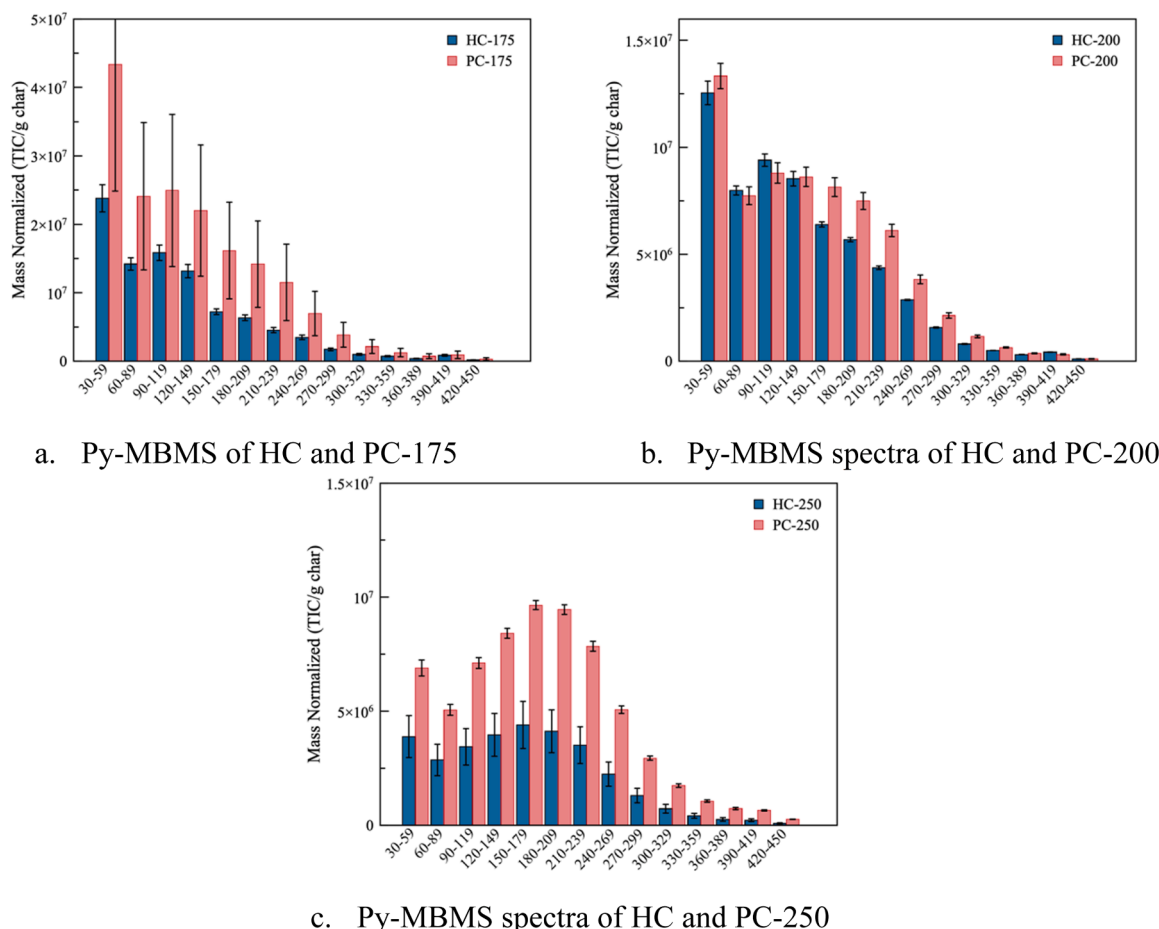


Fig. 5. Py-MBMS spectra of HC and PC samples.

present at much higher intensities in HC and PC-250 than at other temperatures.

Overall, MBMS showed that PCs produce a greater amount of pyrolysis vapors than HCs, which is counterintuitive as PC is expected to produce less pyrolysis vapors due to the extraction of SC. One possible explanation may be the possible presence of solvent still remaining on the surface of the primary char, but this would produce high intensities at *m/z* values typical for the solvent (DCM). However, it is more likely that SC inhibits the cracking of PC during pyrolysis or alters its structure. It appears that the presence of SC causes HC to have a lower surface area, which can be correlated to a lower amount of active sites on the surface of HC wherein pyrolytic reactions can occur, a phenomenon which has been previously reported [38,39]. The surface area of the PCs was found to be an order of magnitude higher than that of the HCs (provided in SI), which further supports the theory that removing SC provides more active sites for pyrolytic reactions to occur, thus producing more pyrolysis vapors.

3.4. Influence of temperature on fast pyrolysis

A representative hydrochar sample, HC-200, was analyzed using a Py-GC-MS-FID instrument at 550°C and 700°C in an attempt to understand how fast pyrolysis temperature influences bio-oil composition (Fig. 6). Raw AP was also pyrolyzed at 550°C to investigate the difference that carbonization has on bio-oils resulting from fast pyrolysis. The raw-AP primarily produced furans and acids during fast pyrolysis, with a total of 17 % of the initial HC identified. The increase in phenol concentration between raw AP and HC-200 points towards the lignin matrix in AP undergoing some decomposition during carbonization, such that when the HC is pyrolyzed, it further degrades into phenolic compounds [40]. This is in agreement with previous studies comparing fast pyrolysis of raw biomass and hydrochar [15]. As 5-HMF is an initial degradation product of glucose, it is likely that more 5-HMF is released during pyrolysis of AP that has been carbonized, as glucose is further broken down relative to raw AP. The increase in hydrocarbons seen during fast pyrolysis at 700°C indicates decomposition of fatty acids and carbonyls at higher temperatures.

3.5. Utilizing fast pyrolysis to recover value-added compounds

The overall motivation of this work was to investigate how the bio-oil composition in a cascading pathway is influenced by the presence of SC on the surface of AP HC, and what compounds could be recovered by fast pyrolysis of hydrochar. Using Py-GC-MS-FID-TCD, it was

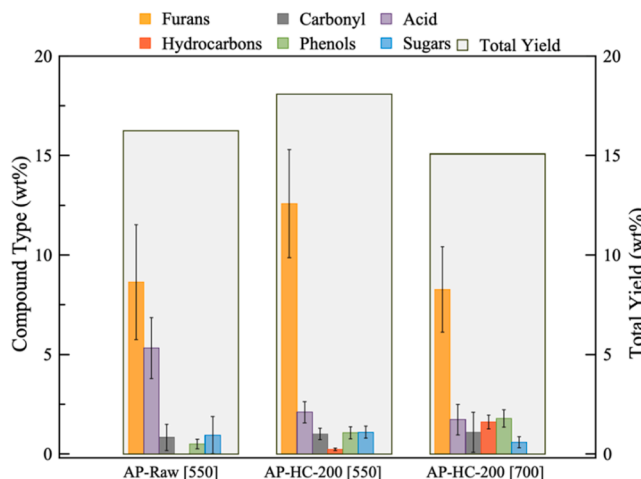


Fig. 6. Composition of vapors produced during fast pyrolysis at 550°C (HC-200, AP-Raw) and 700°C (HC-200). Reported as an average wt% of the hydrochar \pm one standard deviation.

determined that removing the SC directly correlated to a decrease in CO₂ output due to fewer compounds being available to undergo pyrolytic reactions producing CO₂. This was particularly true for AP carbonized at 200 and 250°C. At 175°C, the HC and PC had no significant differences in CO₂ formation but did show differences in CO and furans yield. The HTC yields as well as fast pyrolysis yields, SC composition, and proximate analysis demonstrate that a carbonization temperature of 200°C is sufficient to recover value-added compounds from hydrochar, though 175°C is more optimal for 5-HMF recovery. Recovery of 5-HMF is greater in both SC at 175°C and pyrolysis of HCs. One might suppose that it would be more efficient to separate this 5-HMF via solvent extraction of the HCs rather than bio-oil separation. Future work could probe the recovery efficiencies and selectivities of SC vs bio-oil recovery of 5-HMF to optimize process design.

Some literature suggests that HTC residence time, rather than temperature, may be a more important factor in bio-oil composition, particularly due to increased lignin degradation occurring during longer residence times, ultimately producing more phenols in the bio-oil [15]. While reaction time was beyond the scope of this study (aimed at deconvoluting the impact of SC on pyrolysis of HCs), this reaction variable could be the basis of future work to optimize the conversion of AP to biofuels.

In terms of compound value and recovery, 5-HMF and levulinic acid are regarded as platform chemicals which have value as food additives, precursors to bioplastics, and other functional materials [2,41–43]. As illustrated in Fig. 7, these compounds form at relatively low-temperature HTC (175–220°C), and as HTC temperature increases, they transform to polyfurans.

CO is a syngas component that is often produced using environmentally harmful catalysts, such as Ni-Co bi-metallic catalysts [44] and CeO₂–Ni/CaO-Al₂O₃ catalytic systems [45], but here we produce CO as a byproduct of fast pyrolysis of waste biomass. While tracking gas phase composition was beyond the scope of the present work, future studies could explore how to enhance CO production by building a more precise reaction map. The present work – as seen in Fig. 7 – demonstrates the feasibility and role of SC in recovering valuable bio-oils compounds via pyrolysis of HCs. Through this work, we demonstrated that a combination of secondary char extraction and fast pyrolysis is a potential pathway to extract value-added compounds from agro-industrial waste hydrochar.

4. Conclusions

Apple pomace (AP), a waste biomass from agro-industrial activities, was carbonized at 175, 200, and 250°C and the subsequent hydrochar was subjected to fast pyrolysis before and after secondary char extraction. Hypothesizing that valuable compounds were present in the secondary char, we set out to investigate the devolatilization of these compounds during fast pyrolysis in a quantitative manner. Secondary char (SC) derived from AP was found to have high 5-HMF and levulinic acid content at lower carbonization temperatures. These compounds are valuable platform chemicals that typically are produced from a virgin feedstock. Importantly, the presence of SC decreases the surface area of HC, which ultimately causes an inhibition of pyrolytic reactions. A combination of SC extraction and fast pyrolysis was found to allow for extraction of value-added compounds from hydrochar while maintaining a char material suitable for solid fuel applications.

CRediT authorship contribution statement

Madeline Karod: Writing – original draft, Validation, Methodology, Investigation, Formal analysis, Data curation, Conceptualization. **Jillian Goldfarb:** Writing – review & editing, Supervision, Resources, Funding acquisition, Conceptualization. **Kristiina Iisa:** Writing – review & editing, Supervision, Resources, Funding acquisition, Conceptualization. **Yaseen Elkasabi:** Writing – review & editing, Investigation, Data

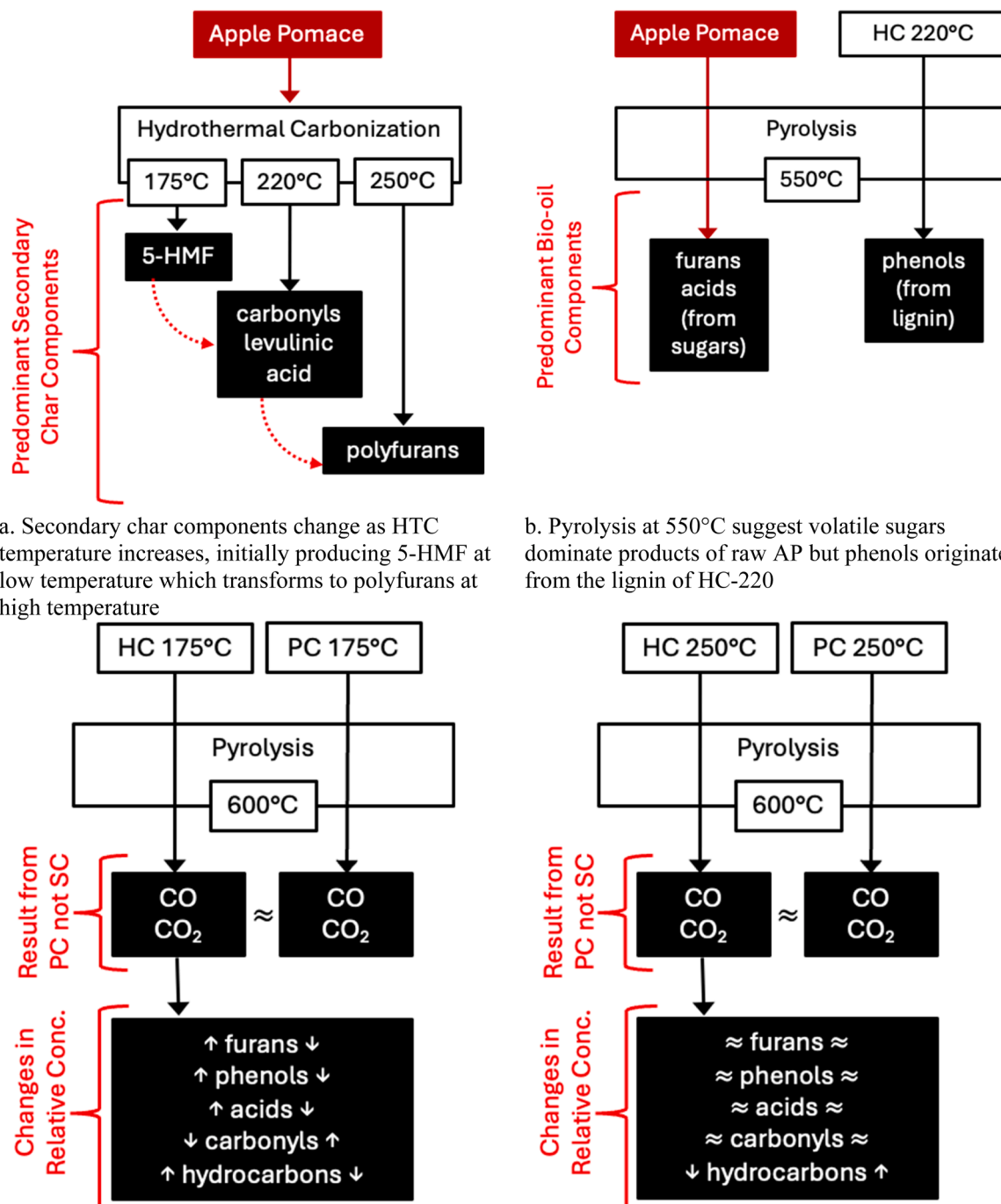


Fig. 7. Overarching reaction pathways observed for AP-HTC and pyrolysis of raw AP, AP-HCs and AP-PCs.

curation. **Kellene A. Orton:** Validation, Methodology, Investigation, Data curation. **Anne E. Harman-Ware:** Writing – review & editing, Supervision, Resources, Investigation, Funding acquisition, Conceptualization. **Charles A. Mullen:** Writing – review & editing, Investigation, Data curation.

Declaration of Competing Interest

The authors declare the following financial interests/personal relationships which may be considered as potential competing interests:

Jillian L. Goldfarb reports financial support was provided by National Science Foundation. Jillian L. Goldfarb reports financial support was provided by USDA-NIFA Hatch Program. If there are other authors, they declare that they have no known competing financial interests or personal relationships that could have appeared to influence the work reported in this paper.

Acknowledgements

This work was supported by a Hatch Grant under accession number

1021398 from the USDA National Institute of Food and Agriculture and from the National Science Foundation (NSF) INTERN-DCL supplement to grant number 2316206. This work was authored in part by the National Renewable Energy Laboratory, operated by Alliance for Sustainable Energy, LLC, for the U.S. Department of Energy (DOE) under Contract No. DE-AC36-08GO28308. Funding provided by the U.S. Department of Energy Office of Energy Efficiency and Renewable Energy Bioenergy Technologies Office. The views expressed in the article do not necessarily represent the views of the DOE or the U.S. Government. The U.S. Government retains and the publisher, by accepting the article for publication, acknowledges that the U.S. Government retains a nonexclusive, paid-up, irrevocable, worldwide license to publish or reproduce the published form of this work, or allow others to do so, for U.S. Government purposes. Mention of trade names or commercial products in this publication is solely for the purpose of providing specific information and does not imply recommendation or endorsement by the U.S. Department of Agriculture. USDA is an equal opportunity provider and employer.

Appendix A. Supporting information

Supplementary data associated with this article can be found in the online version at [doi:10.1016/j.jaat.2024.106868](https://doi.org/10.1016/j.jaat.2024.106868).

Data Availability

Data will be made available on request.

References

- [1] M. Ayaz, D. Feizienė, V. Tilvikienė, K. Akhtar, U. Stulpinaitė, R. Iqbal, Biochar role in the sustainability of agriculture and environment, *Sustainability* (2021), <https://doi.org/10.3390/su13031330>.
- [2] Chang, J. High Value Chemicals and Materials Production Based on Biomass Components Separation. 2014. <https://doi.org/10.1039/9781782620181-00146>.
- [3] K.N. Yogalashmi, D.T. Poorniva, P. Sivashanmugam, S. Kavitha, K.R. Kannah, S. Varjani, S. AdishKumar, G. Kumar, B.J. Rajesh, Lignocellulosic biomass-based pyrolysis: a comprehensive review, *Chemosphere* 286 (2022) 131824, <https://doi.org/10.1016/j.chemosphere.2021.131824>.
- [4] F. Cherubini, The biorefinery concept: using biomass instead of oil for producing energy and chemicals, *Energy Convers. Manag.* 51 (7) (2010) 1412–1421, <https://doi.org/10.1016/j.enconman.2010.01.015>.
- [5] J. Petrović, M. Ercegović, M. Simić, M. Koprivica, J. Dimitrijević, A. Jovanović, J. Janković Pantić, Hydrothermal carbonization of waste biomass: a review of hydrochar preparation and environmental application, *Processes* 12 (1) (2024) 207, <https://doi.org/10.3390/pr12010207>.
- [6] R.J.M. Westerhof, N.J.M. Kuipers, S.R.A. Kersten, W.P.M. Van Swaaij, Controlling the water content of biomass fast pyrolysis oil, *Ind. Eng. Chem. Res.* 46 (26) (2007) 9238–9247, <https://doi.org/10.1021/ie070684k>.
- [7] M. Lucian, M. Volpe, L. Gao, G. Piro, J.L. Goldfarb, L. Fiori, Impact of hydrothermal carbonization conditions on the formation of hydrochars and secondary chars from the organic fraction of municipal solid waste, *Fuel* 233 (2018) 257–268, <https://doi.org/10.1016/j.fuel.2018.06.060>.
- [8] H.S. Kambo, A. Dutta, A comparative review of biochar and hydrochar in terms of production, physico-chemical properties and applications, *Renew. Sustain. Energy Rev.* 45 (2015) 359–378, <https://doi.org/10.1016/j.rser.2015.01.050>.
- [9] M. Pecchi, M. Baratieri, J.L. Goldfarb, A.R. Maag, Effect of solvent and feedstock selection on primary and secondary chars produced via hydrothermal carbonization of food wastes, *Bioreour. Technol.* 348 (2022) 126799, <https://doi.org/10.1016/j.biortech.2022.126799>.
- [10] G. Ischia, J.L. Goldfarb, A. Miotello, L. Fiori, Green solvents to enhance hydrochar quality and clarify effects of secondary char, *Bioreour. Technol.* 388 (2023) 129724, <https://doi.org/10.1016/j.biortech.2023.129724>.
- [11] G. Ischia, M. Cutillo, G. Guella, N. Bazzanella, M. Cazzanelli, M. Orlandi, A. Miotello, L. Fiori, Hydrothermal carbonization of glucose: secondary char properties, reaction pathways, and kinetics, *Chem. Eng. J.* 449 (2022) 137827, <https://doi.org/10.1016/J.CEJ.2022.137827>.
- [12] M. Karod, S.F. Rubin, J.L. Goldfarb, Synergistic improvements in energy recovery and bio-oil quality through integrated thermochemical valorization of agro-industrial waste of varying moisture content, *Bioreour. Technol.* (2023) 130173, <https://doi.org/10.1016/j.biortech.2023.130173>.
- [13] J.L. Adair, M. Karod, J.L. Goldfarb, Addition of in situ clay catalysts at different process points in a cascaded hydrothermal carbonization-pyrolysis process for agro-industrial waste valorization, *Bioreour. Technol.* (2023) 128649, <https://doi.org/10.1016/j.biortech.2023.128649>.
- [14] I. Güdücü, K. Alper, T. Evcil, K. Tekin, H. Ohtani, S. Karagöz, Effects of hydrothermal carbonization on products from fast pyrolysis of cellulose, *J. Energy Inst.* 99 (2021) 299–306, <https://doi.org/10.1016/j.joei.2021.10.004>.
- [15] A. Alcazar-Ruiz, A. Villardon, F. Dorado, Sanchez- Silva, L. Hydrothermal carbonization coupled with fast pyrolysis of almond shells: valorization and production of valuable chemicals, *Waste Manag.* 169 (2023) 112–124, <https://doi.org/10.1016/j.wasman.2023.07.004>.
- [16] H. Tan, C.T. Lee, P.Y. Ong, K.Y. Wong, C.P.C. Bong, C. Li, Y. Gao, A review on the comparison between slow pyrolysis and fast pyrolysis on the quality of lignocellulosic and lignin-based biochar, *IOP Conf. Ser.: Mater. Sci. Eng.* 1051 (1) (2021) 012075, <https://doi.org/10.1088/1757-899X/1051/1/012075>.
- [17] Pechá, B.; García-Perez, M. Chapter 26 - Pyrolysis of Lignocellulosic Biomass: Oil, Char, and Gas. In *Bioenergy*; Dahiyat, A., Ed.; Academic Press: Boston, 2015; pp 413–442. <https://doi.org/10.1016/B978-0-12-407909-0.00026-2>.
- [18] J. Eke, J.A. Onwudili, A.V. Bridgwater, Influence of moisture contents on the fast pyrolysis of tremella fines in a bubbling fluidized bed reactor, *Waste Biomass...* Valor 11 (7) (2020) 3711–3722, <https://doi.org/10.1007/s12649-018-00560-2>.
- [19] M. Pecchi, J.L. Goldfarb, Open-source python module to automate GC-MS data analysis developed in the context of bio-oil analyses, *RSC Sustain* (2024), <https://doi.org/10.1039/D3SU00345K>.
- [20] X. Xing, F. Fan, S. Shi, Y. Xing, Y. Li, X. Zhang, J. Yang, Fuel properties and combustion kinetics of hydrochar prepared by hydrothermal carbonization of corn straw, *BioResources* 11 (4) (2016) 9190–9204, <https://doi.org/10.15376/biores.11.4.9190-9204>.
- [21] H. Shi, N. Mahinpey, A. Aqsha, R. Silbermann, Characterization, thermochemical conversion studies, and heating value modeling of municipal solid waste, *Waste Manag.* 48 (2016) 34–47, <https://doi.org/10.1016/j.wasman.2015.09.036>.
- [22] I. Battonne-Gener, A. Sachse, Determination of the exact microporous volume and bet surface area in hierarchical ZSM-5, *J. Phys. Chem. C.* 123 (7) (2019) 4235–4242, <https://doi.org/10.1021/acs.jpcc.8B11524>.
- [23] J.T. Scanlon, D.E. Willis, Calculation of flame ionization detector relative response factors using the effective carbon number concept, *J. Chromatogr. Sci.* 23 (8) (1985) 333–340, <https://doi.org/10.1093/chromsci/23.8.333>.
- [24] R.M. Happs, B. Addison, C. Doeppke, B.S. Donohoe, M.F. Davis, A.E. Harman-Ware, Comparison of methodologies used to determine aromatic lignin unit ratios in lignocellulosic biomass, *Biotechnol. Biofuels* 14 (1) (2021) 58, <https://doi.org/10.1186/s13068-021-01897-y>.
- [25] R. Sykes, B. Kodrzychki, G. Tuskan, K. Foutz, M. Davis, Within tree variability of lignin composition in populus, *Wood Sci. Technol.* 42 (8) (2008) 649–661, <https://doi.org/10.1007/s00226-008-0199-0>.
- [26] R.W. Sykes, E.L. Gjersing, C.L. Doeppke, M.F. Davis, High-throughput method for determining the sugar content in biomass with pyrolysis molecular beam mass spectrometry, *Bioenerg. Res.* 8 (3) (2015) 964–972, <https://doi.org/10.1007/s12155-015-9610-5>.
- [27] Y. Cao, M. He, S. Dutta, G. Luo, S. Zhang, D.C.W. Tsang, Hydrothermal carbonization and liquefaction for sustainable production of hydrochar and aromatics, *Renew. Sustain. Energy Rev.* 152 (2021) 111722, <https://doi.org/10.1016/j.rser.2021.111722>.
- [28] M. He, Y. Cao, Y. Fan, O. Mašek, J.H. Clark, D.C.W. Tsang, Revealing roles of CO₂ and N₂ in pressurized hydrothermal carbonization process for enhancing energy recovery and carbon sequestration, *Bioreour. Technol.* 385 (2023) 129429, <https://doi.org/10.1016/j.biortech.2023.129429>.
- [29] T.A.H. Nguyen, T.H. Bui, W.S. Guo, H.H. Ngo, Valorization of the aqueous phase from hydrothermal carbonization of different feedstocks: challenges and perspectives, *Chem. Eng. J.* 472 (2023) 144802, <https://doi.org/10.1016/j.cej.2023.144802>.
- [30] C. Mondal, S.K. Pal, B. Samanta, D. Dutta, S. Raj, Analysis and significance of prediction models for higher heating value of coal: an updated review, *J. Therm. Anal. Calor.* 148 (15) (2023) 7521–7538, <https://doi.org/10.1007/s10973-023-12272-4>.
- [31] F.S. Asghari, H. Yoshida, Acid-catalyzed production of 5-hydroxymethyl furfural from d-fructose in subcritical water |, *Ind. Eng. Chem. Res.* 45 (2006) 2163–2173, <https://doi.org/10.1021/ie051088y>.
- [32] N. Baccile, G. Laurent, F. Babonneau, F. Fayon, M.-M. Titirici, M. Antonietti, Structural Characterization of hydrothermal carbon spheres by advanced solid-state ¹³C NMR investigations, *J. Phys. Chem. C.* 113 (22) (2009) 9644–9654, <https://doi.org/10.1021/jp901582x>.
- [33] C. Contreras, H. Tjellström, R.M. Beaudry, Relationships between free and esterified fatty acids and LOX-derived volatiles during ripening in apple, *Postharvest Biol. Technol.* 112 (2016) 105–113, <https://doi.org/10.1016/j.postharbtech.2015.10.009>.
- [34] M. Pecchi, M. Baratieri, A.R. Maag, J.L. Goldfarb, Uncovering the transition between hydrothermal carbonization and liquefaction via secondary char extraction: a case study using food waste, *Waste Manag.* 168 (2023) 281–289, <https://doi.org/10.1016/j.wasman.2023.06.009>.
- [35] J. Liang, H. Lin, C. Li, L. Zhang, S. Zhang, S. Wang, J. Xiang, S. Hu, Y. Wang, X. Hu, Interaction of derivatives of cellulose and lignin in Co-HTC, Co-pyrolysis and Co-activation, *Fuel* 351 (2023) 129033, <https://doi.org/10.1016/j.fuel.2023.129033>.
- [36] J. Paini, V. Benedetti, L. Menin, M. Baratieri, F. Patuzzi, Subcritical water hydrolysis coupled with hydrothermal carbonization for apple pomace integrated cascade valorization, *Bioreour. Technol.* 342 (2021) 125956, <https://doi.org/10.1016/j.biortech.2021.125956>.
- [37] M. Karod, A.H. Hubble, A.R. Maag, Z.A. Pollard, J.L. Goldfarb, Clay-catalyzed in situ pyrolysis of cherry pits for upgraded biofuels and heterogeneous adsorbents as recoverable by-products, *Biomass Convers. Biorefin.* 2022 (2022) 1–13, <https://doi.org/10.1007/S13399-022-02921-3>.

[38] D. Fu, X. Li, W. Li, J. Feng, Catalytic upgrading of coal pyrolysis products over bio-char, *Fuel Process. Technol.* 176 (2018) 240–248, <https://doi.org/10.1016/j.fuproc.2018.04.001>.

[39] K. Ding, Y. Wang, S. Liu, G. Lin, S.S.A. Syed-Hassan, B. Li, X. Hu, Y. Huang, S. Zhang, H. Zhang, Volatile-char interactions during biomass pyrolysis: insight into the activity of chars derived from three major components, *J. Anal. Appl. Pyrolysis* 159 (2021) 105320, <https://doi.org/10.1016/j.jaat.2021.105320>.

[40] X. Chen, Q. Che, S. Li, Z. Liu, H. Yang, Y. Chen, X. Wang, J. Shao, H. Chen, Recent developments in lignocellulosic biomass catalytic fast pyrolysis: strategies for the optimization of bio-oil quality and yield, *Fuel Process. Technol.* 196 (2019) 106180, <https://doi.org/10.1016/j.fuproc.2019.106180>.

[41] A.R. Monteiro, A.P. Battisti, G.A. Valencia, C.J. de Andrade, The production of high-added-value bioproducts from non-conventional biomasses: an overview, *Biomass* 3 (2) (2023) 123–137, <https://doi.org/10.3390/biomass3020009>.

[42] A.V. Ruales-Salcedo, V.H. Grisales-Díaz, R. Morales-Rodríguez, J. Fontalvo, O. A. Prado-Rubio, Chapter 10 - Production of High-Added Value Compounds from Biomass, in: F.I. Gómez Castro, C. Gutiérrez-Antonio (Eds.), In *Biofuels and Biorefining*, Elsevier, 2022, pp. 381–445, <https://doi.org/10.1016/B978-0-12-824116-5.00001-5>.

[43] A. Gandini, A.J.D. Silvestre, C.P. Neto, A.F. Sousa, M. Gomes, The Furan counterpart of poly(Ethylene Terephthalate): an alternative material based on renewable resources, *J. Polym. Sci. Part A: Polym. Chem.* 47 (1) (2009) 295–298, <https://doi.org/10.1002/pola.23130>.

[44] Q. Yu, Y. Jiao, W. Wang, Y. Du, C. Li, J. Yang, J. Lu, Catalytic performance and characterization of Ni-Co Bi-metallic catalysts in n-decane steam reforming: effects of Co addition, *Catalysts* 8 (11) (2018) 518, <https://doi.org/10.3390/catal8110518>.

[45] J. Ashok, S. Kawi, Steam reforming of toluene as a biomass tar model compound over CeO₂ promoted Ni/CaO-Al₂O₃ catalytic systems, *Int. J. Hydrog. Energy* 38 (32) (2013) 13938–13949, <https://doi.org/10.1016/j.ijhydene.2013.08.029>.